

Above the nominal limit performance evaluation of multiwavelength optical code-division multiple-access systems

Elie Inaty

University of Balamand
Faculty of Engineering
Elkoura, North P.O 33
Lebanon
E-mail: elie.inaty@balamand.edu.lb

Robert Raad

Paul Fortier
Université Laval
Faculty of Engineering
Québec, G1K 7P4 Canada

Hossam M. H. Shalaby

University of Alexandria
Department of Electrical Engineering
Faculty of Engineering
Alexandria, Alexandria 21544, Egypt

Abstract. We provide an analysis for the performance of a multiwavelength optical code-division multiple-access (MW-OCDMA) network when the system is working above the nominal transmission rate limit imposed by passive encoding-decoding operation. We address the problem of overlapping in such a system and how it can directly affect the bit error rate (BER). A unified mathematical framework is presented under the assumption of one-coincidence sequences with nonrepeating wavelengths. A closed form expression of the multiple access interference limited BER is provided as a function of different system parameters. Results show that the performance of the MW-OCDMA system can be critically affected when working above the nominal limit, an event that can happen when the network operates at a high transmission rate. In addition, the impact of the derived error probability on the performance of two newly proposed medium access control (MAC) protocols, the S-ALOHA and the R^3T , is also investigated. It is shown that for low transmission rates, the S-ALOHA is better than the R^3T , while the R^3T is better at very high transmission rates. In general, it is postulated that the R^3T protocol suffers a higher delay mainly because of the presence of additional modes. © 2009 Society of Photo-Optical Instrumentation Engineers. [DOI: 10.1117/1.3099613]

Subject terms: multiwavelength; optical code-division multiple access; fiber Bragg grating; multirate; overlapping coefficient; one-coincidence sequences; S-ALOHA; R^3T .

Paper 080820R received Oct. 20, 2008; revised manuscript received Jan. 22, 2009; accepted for publication Jan. 22, 2009; published online Apr. 1, 2009.

1 Introduction

Lately, multiwavelength optical code-division multiple-access (MW-OCDMA) has received considerable attention as a multiple access scheme for optical local area networks due to its flexibility and diversity.¹⁻³ In addition, multiservices supporting multirate transmission using MW-OCDMA are now feasible due to the rapid evolution of fiber optic technology that offers ultrawide optical bandwidth capable of handling fast transmission rates. Toward this target, the bit-error-rate (BER) analysis of such a system is a crucial task.³

MW-OCDMA has been proposed and discussed in numerous works.^{4,5} In addition, the BER has been derived and studied in detail.^{1,2} In Ref. 4, we have proposed a multirate MW-OCDMA system using fiber Bragg grating and variable processing gain (PG). The idea was to respect the total round-trip time for light from a data bit to go through the encoder. One of the key issues emphasized in Ref. 4 is the difference between passive optical CDMA and its electrical active counterpart. In fact, it has been argued that in active CDMA systems there is a one-to-one correspondence between the transmitted symbol duration and the PG. On the other hand, this one-to-one relation does not exist in passive optical CDMA systems. For instance, decreasing the

bit duration will not affect the symbol duration at the output of the optical encoder. Therefore, for a fixed PG, increasing the link transmission rate beyond a given value, known as the nominal rate, leads to bit overlap at the output of the encoder. In Ref. 4, the general problem we have considered is how much we can increase the transmission rates of different classes of traffic beyond the nominal permitted rates to optimize performance to meet the quality of service (QoS) requirements. The QoS requirement has been taken to be the signal-to-interference ratio (SIR).

Although the SIR is considered to be a good QoS index, some network managers prefer the BER as a more reliable and exact QoS measure. In Refs. 2 and 5, the BER for the MW-OCDMA system has been presented in detail when the system works below the nominal limit. This means that sequences with ideal cross-correlation function of a maximum one were assumed. The probability of having one hit between two code sequences was obtained and the BER is derived using the binomial distribution. On the other hand, in Ref. 1, although the performance analysis of code sequences with arbitrary cross-correlation values is considered, the explicit equation of the probability of having more than one hit between two code sequences was not presented. Only the probability of having one and two hits was shown in Ref. 6 where a special family of nonideal optical orthogonal codes was analyzed.

In this work, we try to analyze the performance of the

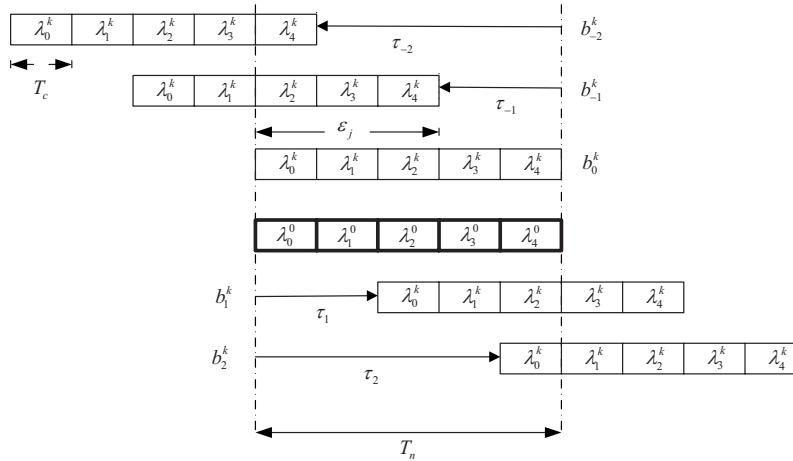


Fig. 1 The concept of overlapping among the bits, showing the effect of the overlapping coefficient ϵ_j on their transmission rate.

MW-OCDMA system when the network is working above the nominal rate limit imposed by passive encoding-decoding operation. A unified mathematical framework is presented in a way that the probability of having any number of hits between sequences can be obtained. We focus on the problem of overlapping in such a system and how it can mathematically affect the expression of the BER. Using this expression, the performance of the MW-OCDMA system is investigated in packet optical networks using two newly proposed medium access control (MAC) protocols, the R^3T^7 and the S-ALOHA.⁸

Following the introduction, the work is structured as follows. Section 2 introduces the system model. The effect of overlapping on frequency hits and interference quantification is discussed in Sec. 3. Section 4 presents the BER analysis assuming multiple access interference (MAI)-limited noise effect. Numerical results are covered in Sec. 5. Finally, the conclusion is presented in Sec. 6.

2 System Model

Consider an MW-OCDMA communication network that supports M users, sharing the same optical medium in a star architecture.² We consider that all users are transmitting their data at the same transmission rate and have the same processing gain G . Encoding and decoding are achieved passively using a sequence of fiber Bragg gratings (FBGs). The gratings spectrally and temporally slice an incoming broadband pulse into several components equally spaced at chip intervals $T_c = 2n_g L_c / c$.⁴ L_c represents the grating length, assuming that the grating's temporal response is an ideal square wave function, c is the speed of light, and n_g is the group index. The chip duration and the number of gratings will establish the nominal bit rate of the system, i.e., the round-trip time of light, from a given transmitted bit, to be totally reflected from the encoder. This nominal bit duration in a structure of G gratings is given by $T_n = 2Gn_g L_c / c$, which is normally greater or equal to the transmission bit time period. The corresponding nominal rate is $R_n = 1/T_n$.

Due to the linearity of the gratings [first in first out (FIFO)], hence the linearity of the encoder-decoder set,

when the data rate increases beyond R_n , multibits will be coded during the time period T_n and transmitted. At a given receiver, the decoder observes practically multicode, which are delayed according to the transmission rate of the source, as shown in Fig. 1. When user k transmits using rate $R_j > R_n$, it introduces a bit overlap coefficient ϵ_j , according to which the new transmission rate is related to the nominal rate through the following equation,

$$R_j = \frac{G}{G - \epsilon} R_n, \tag{1}$$

where $0 \leq \epsilon_j \leq G - 1$. This implies that $R^{(\ell)} \leq R_j \leq R^{(u)}$, where $R^{(\ell)} = R_n$ and $R^{(u)} = GR_n$ are the lower and upper data rates common to all users, respectively. Also, we assume that the system is chip synchronous and of discrete rate variation. Furthermore, all users transmit with equal power and have the same overlapping coefficient. In the example presented in Fig. 1, the concept of overlapping is illustrated among six bits of $G=5$ and the overlapping coefficient is $\epsilon_j=3$, which means that there are three chips in each OCDMA-coded bit that overlap with three chips of the other bits. This, in turn, augments the overall transmission rate of the users involved in this class from three bits after $3T_n$ to five bits. In general, the overlapping coefficient represents the number of overlapped chips among consecutive bits.

In Fig. 1 we define λ_i^k as the wavelength of the k 'th user at the i 'th time slot, which is reflected by the i 'th FBG. From Fig. 1, the optical bit stream can be seen to be serial-to-parallel converted to v optical pulses. Because the bit b_X^k from the v bits is delayed by $\tau_X = X(G - \epsilon_j)$, this suggests that the channel model, as seen by the desired receiver, can be represented as a tapped delay line with tap spacing of $\tau_{-1} = -(G - \epsilon_j)$ from the left and $\tau_1 = (G - \epsilon_j)$ from the right. The tap weight coefficients $b_X^k \in \{0, 1\}$ depend on whether the transmitted bit is zero or one.

Accordingly, the average cross-correlation function between two one-coincidence sequences⁹⁻¹¹ has been obtained in Ref. 4 and is given by

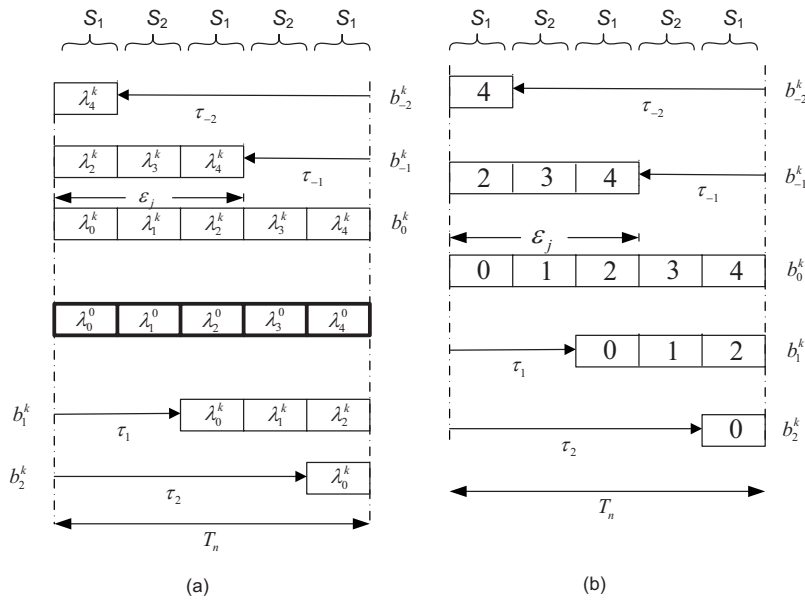


Fig. 2 (a) Code interference pattern and (b) the corresponding indices of the interference sequences.

$$\bar{R}(G, \varepsilon_j) = \frac{1}{2F} [G + (G + \varepsilon_j)X - (G - \varepsilon_j)X^2], \quad (2)$$

where

$$X = \left[\frac{\varepsilon_j}{G - \varepsilon_j} \right], \quad (3)$$

and F is the total number of available wavelengths from which the code is generated.^{10,11}

Although we have been able to study the performance of the multirate MW-OCDMA in Ref. 4, the work was based on the average of the cross-correlation function assuming one-coincidence sequences. In this work, we attempt to evaluate the performance of this system probabilistically in a way to obtain a closed form solution of the exact BER analysis of this system.

3 Multiple Access Interference Identification

As shown in Ref. 4, increasing the transmission rate will increase the overlapping coefficient, and therefore will induce more interference. Throughout this section we try to study and quantify the effect of overlapping for one-coincidence sequences with nonrepeating frequencies.¹⁰

3.1 Overlapped Interference Sequences Identification

Consider an interferer user k with (G, ε_j) as the one presented in Fig. 1. During the autocorrelation process, we look only to the nominal period T_n . Therefore, the interfering sequence as seen by the desired user's receiver is shown in Fig. 2. In this figure, we notice many important aspects. The first one is that at every chip position, there is an interfering pattern that forms a sequence with different elements like $S_1 = \{\lambda_0^k, \lambda_2^k, \lambda_4^k\}$. The second observation is that each interfering sequence is repeated multiple times at different chip positions.

Lemma 1. In an overlapped optical CDMA system, let an interferer with (G, ε_j) . At the desired correlation receiver end, and during the nominal observation time period T_n , the observed interfering sequences are subdivided into two groups. In the first group there are m_1 sequences of length,

$$N_1 = \left\lceil \frac{G}{G - \varepsilon_j} \right\rceil, \quad (4)$$

with

$$m_1 = G - (G - \varepsilon_j) \left\lceil \frac{\varepsilon_j}{G - \varepsilon_j} \right\rceil. \quad (5)$$

The remaining

$$m_2 = (G - \varepsilon_j) \left\lceil \frac{\varepsilon_j}{G - \varepsilon_j} \right\rceil - \varepsilon_j, \quad (6)$$

sequences form the second group in which each sequence is of length

$$N_2 = \left\lceil \frac{\varepsilon_j}{G - \varepsilon_j} \right\rceil. \quad (7)$$

Proof. Consider the wavelength index of the interfering wavelength at the i 'th time slot to be i . Thus, the interfering code can be represented by a sequence of positive integers $S = \{1, 2, 3, \dots, G\}$. For an interferer with an overlapping coefficient ε_j , the desired user's correlation receiver observes, at the i 'th time slot, a chain sequence S_i with $S_i \subset S$. Let α_i to be the smallest element in S_i . Notice that the step size in S_i is the bit delay $\tau = (G - \varepsilon_j)$. In addition, it is clear that the total number of distinct interfering sequences is τ .

Therefore, each interfering sequence $S_i \forall i \in \{1, 2, \dots, \tau\}$ can be completely characterized by α_i and τ as follows

$$\alpha_i = \beta_i(n) \bmod(\tau), \tag{8}$$

where $\beta_i(n)$ is the n 'th element in S_i and $n \in \mathbb{N}^+$, the maximum of which is N_i , which needs to be determined for every sequence.

The first τ interfering sequences completely identify the overall interfering patterns, because the patterns are repeated every τ time slots. Thus, we can write $\alpha_i = i \forall i \in \{1, 2, \dots, \tau\}$. Using Eq. (8), N_i can be written as

$$N_i = \frac{\beta_i(n) - i}{\tau} + 1. \tag{9}$$

S_1 possesses the highest length N_1 , while S_τ has the smallest length N_τ . Using Eq. (9), we define the length difference Δ to be

$$\Delta = N_1 - N_\tau = \frac{\beta_1(N_1) - \beta_\tau(N_\tau) + \tau - 1}{\tau}. \tag{10}$$

Knowing that $\beta_1(N_1) - \beta_\tau(N_\tau) = 1$, we obtain $\Delta = 1$. This means that the τ different interfering sequences can be classified into two groups that differ between each other by a length difference of one. The first group of sequences with the highest length is imposed by the last overlapped bit of index X given in Eq. (3). The number of sequences in this group is given by

$$m_1 = G - X\tau = G - (G - \varepsilon_j) \left\lceil \frac{\varepsilon_j}{G - \varepsilon_j} \right\rceil,$$

which proves Eq. (5). Using $\beta_i(N_i) = X\tau + 1$ in Eq. (9), we obtain

$$N_1 = X + 1 = \left\lceil \frac{G}{G - \varepsilon_j} \right\rceil,$$

which proves Eq. (4). Obviously the remaining

$$m_2 = m - m_1 = (G - \varepsilon_j) \left\lceil \frac{\varepsilon_j}{G - \varepsilon_j} \right\rceil - \varepsilon_j$$

sequences have length

$$N_2 = N_1 - 1 = \left\lceil \frac{\varepsilon_j}{G - \varepsilon_j} \right\rceil,$$

which prove Eqs. (6) and (7), respectively.

Lemma 1 is very important in the sense that it enables us to quantify the effect of overlapping on the interference patterns at a given receiver.

3.2 Hits Quantification Due to Overlap

By observing Fig. 2, we can notice clearly that there are two different kinds of interfering sequences, $S_1 = \{\lambda_0^k, \lambda_2^k, \lambda_4^k\}$ and $S_2 = \{\lambda_1^k, \lambda_3^k\}$. In addition, S_1 is repeated

three times and S_2 is repeated two times. Thus, to study the contribution of S_1 on the MAI, we need to compare it with the desired user wavelengths where it is present. Therefore, we need to compare $S_1 = \{\lambda_0^k, \lambda_2^k, \lambda_4^k\}$ with $d_1 = \{\lambda_0^0, \lambda_2^0, \lambda_4^0\}$. The same argument can be applied to the sequence S_2 where we need to compare $S_2 = \{\lambda_1^k, \lambda_3^k\}$ to $d_2 = \{\lambda_1^0, \lambda_3^0\}$.

Take for example S_1 and d_1 . It is clear that there are up to three possible matching events between elements in S_1 and elements in d_1 . Thus one element in S_1 can be in d_1 , two elements in S_1 can be in d_1 , or three elements in S_1 can match with three elements in d_1 . Each of those events represents the number of hits the interfering sequence S_1 induces at the desired user's receiver. The probabilities of those events are critical in deriving the BER of this system.

In general, consider an interfering sequence S_i and the desired sequence d_i , both of them with length N_i , where N_i can be obtained using Lemma 1. The probability that S_i causes i hits in the cross-correlation function is the probability that exactly i terms in S_i match with i terms in d_i . If we are selecting N_i wavelengths at a time from a set of F possible wavelengths, then the probability of having exactly i wavelengths match with the sequence d_i of length N_i and $N_i - i$ not matching can be written as

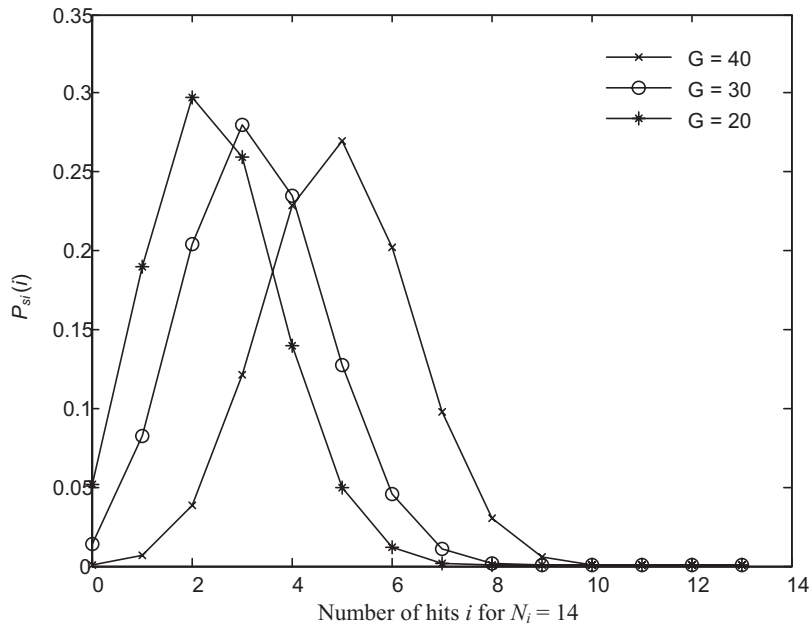
$$P_{S_i}(i) = \frac{\binom{N_i}{i} \binom{F - N_i}{N_i - i}}{\binom{F}{N_i}} \quad \forall 0 \leq i \leq N_i < F, \tag{11}$$

where $\binom{x}{i}$ is the binomial coefficient. All the permutations of a given combination s_i will result in i hits, assuming that there are exactly i wavelengths in s_i that match with i wavelengths in d_i .

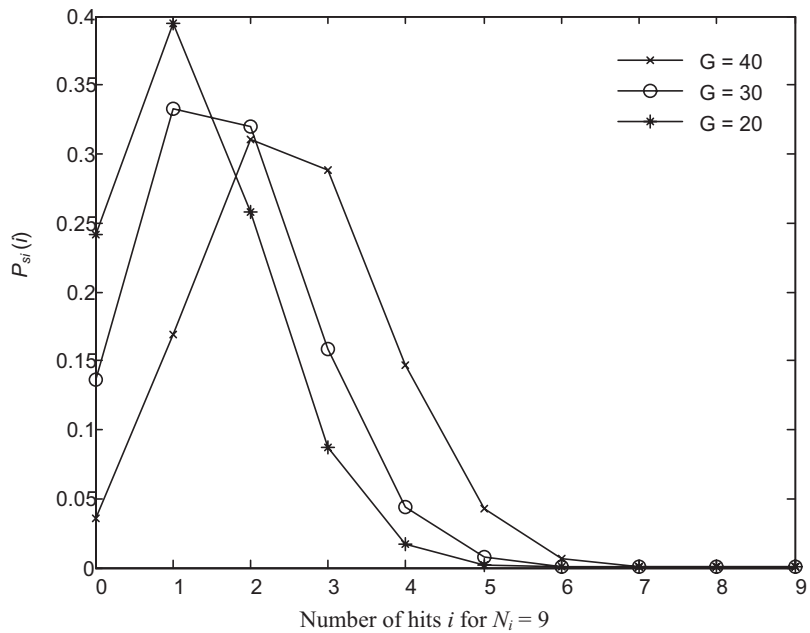
An illustration of Eq. (11) is shown in Fig. 3, where we plot the probability that the interfering sequence S_i causes i hits versus i for $N_i = 14$ [Fig. 3(a)] and $N_i = 9$ [Fig. 3(b)] and for different values of G . In addition, we assume that $F = 2G$. Notice that as the PG increases, although the probability of having a smaller number of hits decreases, the probability of a higher number of hits increases. This result is not like we expect, as in the case of unoverlapped systems where the length of the interfering sequence is always one and increasing the PG will lead to a decrease in the probability of hits.

4 Multiple Access Interference Limited Bit Error Rate Analysis

Obviously, it is clear that due to the overlapping process, the assumption of one-coincidence sequences will not guarantee the upper bound on the number of hits to be one, as in classical nonoverlapped systems. In fact, the number of hits between two overlapped code sequences is related to the number of interference sequences and the size of each of those sequences. For example, if we return to the case studied and shown in Fig. 2, both interference sequences $S_1 = \{\lambda_0^k, \lambda_2^k, \lambda_4^k\}$ and $S_2 = \{\lambda_1^k, \lambda_3^k\}$ may cause up to five hits with different probabilities of occurrence. The importance of our work is to highlight those differences and to emphasize their effect on the performance evaluation of the system.



(a)



(b)

Fig. 3 The probability that the sequence S_i causes i hits in the cross-correlation function.

To evaluate the performance of the overlapped system, we need to find the probability that two overlapped codes have one, two, or p hits in their cross-correlation function, such that $p \leq G$. We proceed by showing the case presented in Fig. 2. The interference pattern of this example can be simplified to two sequences of interference or hits $[H_1, H_2]$, which represent the number of possible hits caused by interference sequences S_1 and S_2 , respectively. In our example, H_1 can take four possible values $H_1 = \{0, 1, 2, 3\}$, and H_2 can take three possible values $H_2 = \{0, 1, 2\}$ with different probabilities as revealed in Fig. 4.

Different possibilities of hits caused by both sequences

H_1	H_2	H_1	H_2	H_1	H_2	H_1	H_2
0	0	1	0	2	0	3	0
0	1	1	1	2	1	3	1
0	2	1	2	2	2	3	2

Fig. 4 Different possible hit configurations.

are presented in Fig. 4. According to Fig. 4, to compute the probability of having j hits from a given interferer, we have to find the probability of having $H_1+H_2=s$. For example, the probability of having three hits is obtained as follows;

$$\begin{aligned} q_3 &= \Pr\{(H_1 = 3 \cap H_2 = 0) \cup (H_1 = 2 \cap H_2 = 1) \cup (H_1 \\ &= 1 \cap H_2 = 2)\} = \frac{1}{(N_1 + 1)(N_2 + 1)} \{P_{S_1}(3) \cdot P_{S_2}(0) \\ &+ P_{S_1}(2) \cdot P_{S_2}(1) + P_{S_1}(1) \cdot P_{S_2}(2)\} \\ &= \frac{1}{(N_1 + 1)(N_2 + 1)} \sum_i \{P_{S_1}(j) \cdot P_{S_2}(k)\}, \end{aligned} \quad (12)$$

where $N_1=3$ and $N_2=2$ are the lengths of the sequences S_1 and S_2 , respectively. In addition, the parameters j and k are chosen such that $j+k=3$, $\forall j=\{0,1,2,3\}$, and $k=\{0,1,2\}$. The parameter i represents the number of cases satisfying $j+k=3$.

Lemma 2. Consider two positive integer numbers $i \in \{0,1,\dots,N_1\}$ and $j \in \{0,1,\dots,N_2\}$ with $N_1 < N_2$. The number of possible couples (i,j) , Λ , satisfying $i+j=s$, $\forall s \in \{0,1,\dots,N_1+N_2\}$, is given by

$$\Lambda = \begin{cases} s+1, & \text{if } 0 \leq s \leq N_1 \\ N_1+1, & \text{if } N_1 < s \leq N_2 \\ N_1+N_2-s+1, & \text{if } N_2 < s \leq N_1+N_2 \end{cases}. \quad (13)$$

Proof. To achieve $s=i+j$, the general form of (i,j) can always be written as $(i,s-i)$. Therefore, the problem under consideration is simplified to find the bounds of i . Consider first that $0 \leq s \leq N_1$. In this case, i can be incremented from zero to s . This in turn shows that the number of possibilities is $s+1$. On the other hand, if $N_1 < s \leq N_2$, i can be incremented from zero to N_1 . Thus, the total number of possibilities is N_1+1 . The last possible range of s is $N_2 < s \leq N_1+N_2$. In this case, i must start with $s-N_2$ and be incremented until N_1+1 . The total number of steps is thus N_1+N_2-s+1 , which completes the proof of the Lemma.

Using Lemma 2, we can generalize Eq. (12) to the case of any number of hits. Therefore, the probability of having s hits is given by

$$q_s = \frac{1}{(N_1 + 1)(N_2 + 1)} \sum_{i=a}^b P_{S_1}(s-i) \cdot P_{S_2}(i), \quad (14)$$

where

$$(a,b) = \begin{cases} (0,s), & \text{for } 0 \leq s \leq N_1 \\ (0,N_1), & \text{for } N_1 < s \leq N_2 \\ (s-N_1,N_2), & \text{for } N_2 < s \leq N_1+N_2 \end{cases}. \quad (15)$$

In addition, using Lemma 2, we can generalize the probability of having s hits given in Eqs. (14) and (15) to any number of interfering sequences. For example, assume that the number of interfering sequences is four. Thus, let $i \in \{0,1,\dots,N_1\}$, $j \in \{0,1,\dots,N_2\}$, $k \in \{0,1,\dots,N_3\}$, and t

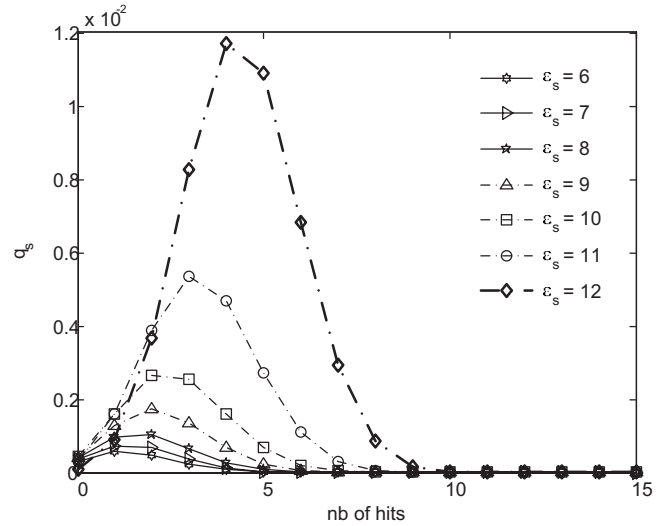


Fig. 5 The probability mass function of the number of hits for different values of the overlapping coefficient ϵ_s .

$= \{0,1,\dots,N_4\}$ with $N_1 \leq N_2 \leq N_3 \leq N_4$. The distribution of the number of hits is the probability of having s hits, and is given by

$$\begin{aligned} q_s &= \frac{1}{\prod_{i=1}^4 (N_i + 1)} \sum_{t=0}^{N_4} \sum_{k=0}^{N_3} \sum_{i=a}^b P_{S_1}(s-k-t \\ &- i) \cdot P_{S_2}(i) \cdot P_{S_3}(k) \cdot P_{S_4}(t), \end{aligned} \quad (16)$$

where

$$(a,b) = \begin{cases} (0,s-k-t), & \text{for } 0 \leq s-k-t \leq N_1 \\ (0,N_1), & \text{for } N_1 < s-k-t \leq N_2 \\ (s-k-t-N_1,N_2), & \text{for } N_2 < s-k-t \leq N_1+N_2 \end{cases}. \quad (17)$$

Figure 5 shows the distribution of the number of hits when $G=15$, $F=18$, and for different values of ϵ_s . It is clear that when the system works above the nominal limit, it may induce more than one hit, even if the codes used are one-coincidence codes. This in turn will drastically influence the probability of error of the system. Notice that, as we further increase the transmission rate, the probability of having larger numbers of hits becomes higher, thus increasing the MAI.

Having obtained in Eq. (16) the probability of s hits in the cross-correlation function, we can now compute the MAI-limited BER when the system is working above the nominal limit. Let Z , TH , and M denote the cross-correlation value seen by the desired receiver, the decision threshold, and the total number of simultaneous users in the system, respectively. Obviously, an error occurs whenever the transmitted data bit is zero, but the interference at the desired receiver results in $Z > TH$. Thus, the probability of error is given by

$$P_e = \Pr(\text{error}/M \text{ simultaneous users}) = \frac{1}{2} \Pr(Z) \geq TH/M \text{ users and the desired user sent 0),} \quad (18)$$

where we have assumed that the data bit zeros and ones are equiprobable.

Assume that S is the total number of interfering pulses in the cross-correlation function and that each interfering user may contribute up to S pulses in it. Let l_j to be the number of interfering users that has a cross-correlation value j . Then, the probability of having $\{l_1, l_2, \dots, l_S\}$ interfering users follows a multinomial probability density function¹² and it is given by

$$\Pr(l_1, l_2, \dots, l_S) = \frac{(M-1)!}{(\prod_{j=1}^S l_j!)(M-1-\sum_{j=1}^S l_j)!} \left(\prod_{j=1}^S q_j^{l_j} \right) \times \left(1 - \sum_{j=1}^S q_j \right)^{(M-1-\sum_{j=1}^S l_j)}, \quad (19)$$

where q_j is given in Eqs. (16) and (17). Using Eq. (19) in Eq. (18), we obtain

$$P_e = \frac{1}{2} - \frac{1}{2} \sum_{l_1=0}^{TH-1} \cdot \sum_{l_2=0}^{[TH-1-l_1/2]} \cdots \sum_{l_S=0}^{[(TH-1-\sum_{j=1}^{S-1} l_j)/S]} \Pr(l_1, l_2, \dots, l_S). \quad (20)$$

5 Numerical Results

Throughout this section, we try to study and discuss the previously derived equations using numerical evaluation. In addition, the impact of the exact BER analysis on the performance of two newly proposed MAC protocols, the S-ALOHA and R^3T protocols, is also investigated. For a complete and detailed discussion of both protocols, the reader is invited to refer to Refs. 7 and 8. Throughout this section, we assume that the total number of stations is $M=15$, and the processing gain is $G=15$.

In Fig. 6, we show the error probability as a function of the number of users M and for different values of the overlapping coefficient ε when the number of available wavelengths is double the code length [Fig. 6(a)]¹⁰ and when the number of available wavelengths is equal to the code length [Fig. 6(b)]⁹. The error probability increases when increasing M , as expected. In addition, the error probability increases when increasing the transmission rate, therefore increasing ε . This is due to the increase in the probability of hits. Notice the importance of the number of available frequencies F on the performance of MW-OCDMA by observing that the probability of error shown in Fig. 6(a) for $F=2G$ is much lower than that presented in Fig. 6(b) where $F=G$. This means that code families that provide a flexibility of choosing F like the one in Ref. 10 can offer better performance than that in which $F=G$.⁹

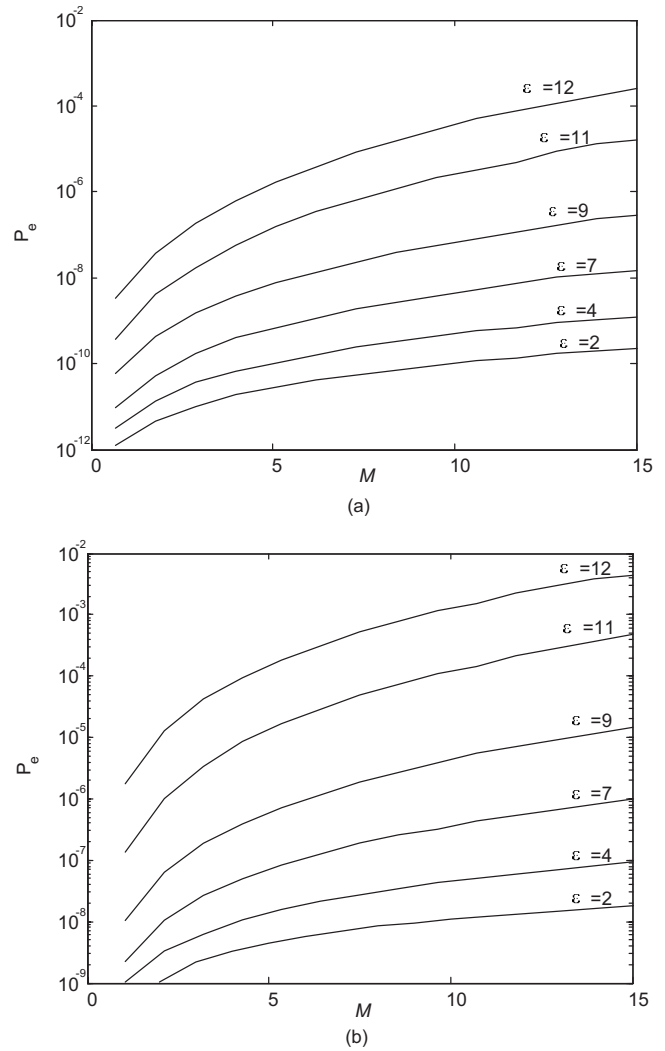


Fig. 6 Probability of error versus the number of users M for different values of ε and when: (a) $F=2G$ and (b) $F=G$.

In the following simulation, we assume that the packet length under S-ALOHA protocol is $L=100$ bits/time slot and the message is one packet. While equivalently, under the R^3T protocol the packet length is one bit/time slot and $L=100$ designates the message length in packets. Note that there is a correspondence between A and P_r . In S-ALOHA, when a terminal enters the backlogged mode, it cannot generate new packets until all the accumulated ones in the system's buffer are retransmitted. Consequently, the offered traffic varies according to the retransmission probability P_r . Meanwhile, in R^3T , the terminal in case of transmission failure retransmits the last unsuccessful t packets with the same transmission probability (user's activity) A , which varies the offered traffic. For S-ALOHA, we assume $P_r=0.6$, whereas for R^3T , we assume $A=0.6$, the time out duration $\tau_o=1$ time slot, and the two-way propagation delay is $t=2$ time slots.

The throughput of both systems is presented in Fig. 7. In Fig. 7(a) we present the throughput versus the offered traffic using a detection threshold $TH=G/2$, while Fig. 7(b) shows the throughput when using the optimal detection

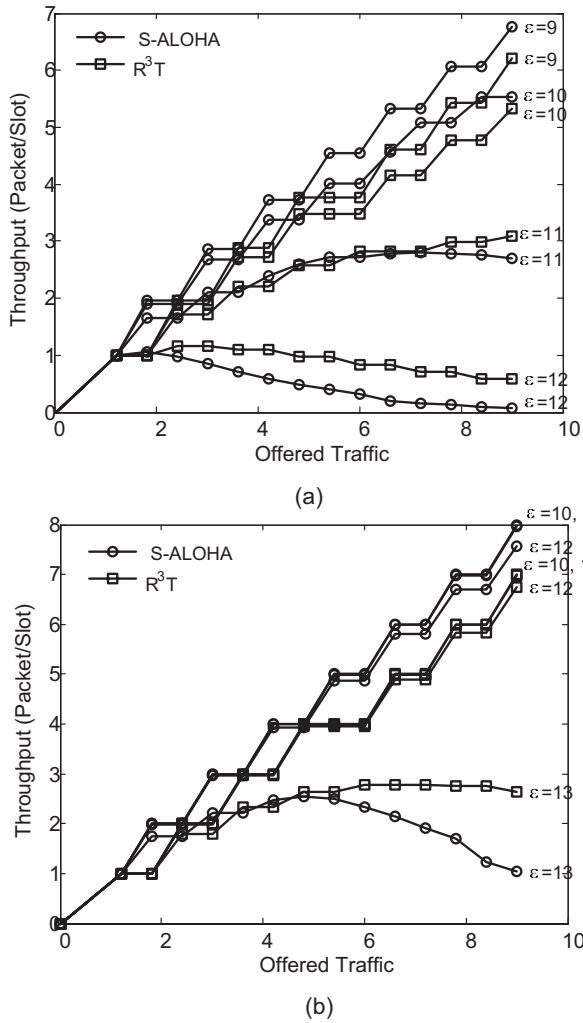


Fig. 7 Throughput versus the offered traffic of the MW-OCDMA system under the two MAC protocols: S-ALOHA and R^3T and using (a) nonoptimal detection threshold and (b) optimal detection threshold.

threshold. The impact of the detection threshold is very obvious in the sense that there is a noticeable increase in the network throughput when using the optimal detection threshold.

It is clear that, for high overlapping coefficients, the R^3T protocol exhibits higher throughput than the S-ALOHA protocol, while the throughputs of the S-ALOHA protocol are higher than that of the R^3T when ϵ is relatively small. For the S-ALOHA protocol, when using the optimal detection threshold, the system reaches its maximum throughput of eight packets per time slot for $\epsilon < 10$. On the other hand, the R^3T protocol reaches its maximum throughput of seven packets per time slot for $\epsilon < 10$, as revealed by Fig. 7(b).

As the transmission rate increases, the throughput of the S-ALOHA decreases compared to that of the R^3T . This means that the R^3T protocol can manage higher-rate users better than the S-ALOHA due to its efficient administration of erroneous packets using the “Round Robin” and the “Go-back- n ” protocols.

In Fig. 8 we present the average packet delay versus the system throughput, operating under the two mentioned protocols using the optimal detection threshold as in Fig. 8(b),

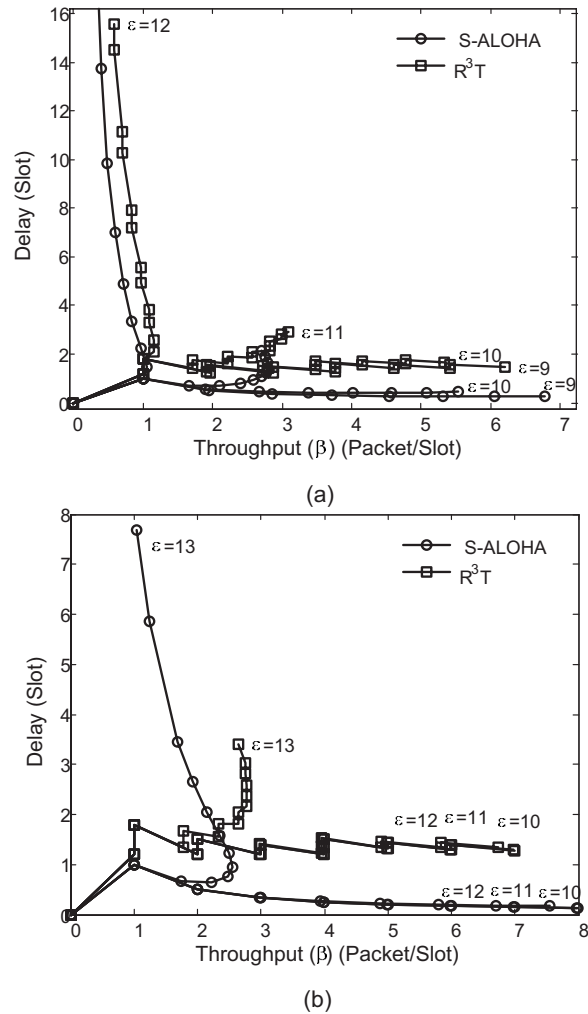


Fig. 8 Average packet delay versus the throughput of the MW-OCDMA system under the two MAC protocols: S-ALOHA and R^3T and using (a) nonoptimal detection threshold and (b) optimal detection threshold.

and a nonoptimal detection threshold as in Fig. 8(a), respectively. Here again we remark that the R^3T protocol exhibits higher delay at low throughput for relatively small values of ϵ . On the other hand, the S-ALOHA protocol exhibits higher delay at low throughput for higher values of ϵ . Notice that when using the optimal detection threshold, the S-ALOHA achieves its maximum throughput with virtually no delay when $\epsilon < 10$, while the R^3T protocol takes around one time slot to achieve its maximum throughput. This is due to the use of the “Go-back- n ” protocol.

By comparing the performance of the MW-OCDMA system under both protocols, we notice that for low transmission rates, the S-ALOHA is better than the R^3T , while the R^3T is better at very high transmission rates.

6 Conclusion

An analysis of the performance of the MW-OCDMA network when the system is working above the nominal transmission rate limit is provided. A unified mathematical framework is presented under the assumption of one-coincidence sequences with nonrepeating wavelengths. A

closed form expression of the BER is derived. Results show that the performance of the MW-OCDMA system may be critically affected when working above the nominal limit. In addition, the impact of the derived error probability on the performance of two newly proposed MAC protocols, the S-ALOHA and the R^3T , is also investigated. It is shown that for low transmission rates, the S-ALOHA is better than the R^3T , while the R^3T is better at very high transmission rates. However, in general, the R^3T protocol suffers a higher delay because of the presence of additional modes.

Acknowledgment

This work was supported in part by the Lebanese CNRS.

References

1. C. C. Hsu, G. C. Yang, and W. C. Kwong, "Performance analysis of 2-D optical codes with arbitrary cross-correlation values under the chip-asynchronous assumption," *IEEE Commun. Lett.* **11**(2), 170–172 (2007).
2. T. M. Bazan, D. Harle, and I. Andonovic, "Performance analysis of 2-D time-wavelength OCDMA systems with coherent light sources: code design considerations," *J. Lightwave Technol.* **24**(10), 3583–3589 (2006).
3. H. M. H. Shalaby, "Complexities, error probabilities, and capacities of optical OOK-CDMA communication systems," *IEEE Trans. Commun.* **50**(12), 2009–2017 (2002).
4. E. Inaty, H. M. H. Shalaby, and P. Fortier, "On the cutoff rate of a multiclass OFFH-CDMA system," *IEEE Trans. Commun.* **53**(2), 323–334 (2005).
5. G. C. Yang and W. C. Kwong, *Prime Codes with Applications to CDMA Optical and Wireless Networks*, Artech house, New York (2002).
6. C. S. Weng and J. Wu, "Optical orthogonal codes with nonideal cross correlation," *J. Lightwave Technol.* **19**, 1856–1863 (2001).
7. H. M. H. Shalaby, "Performance analysis of an optical CDMA random access protocol," *J. Lightwave Technol.* **22**, 1233–1241 (2004).
8. R. Raad, E. Inaty, P. Fortier, and H. M. H. Shalaby, "Optical S-ALOHA/CDMA system for multirate applications: architecture, performance evaluation, and system stability," *J. Lightwave Technol.* **24**(5), 1968–1977 (2006).
9. L. D. Wronski, R. Hossain, and A. Albicki, "Extended hyperbolic congruential frequency hop code: generation and bounds for cross- and auto-ambiguity function," *IEEE Trans. Commun.* **44**(3), 301–305 (1996).
10. L. Bin, "One-coincidence sequences with specified distance between adjacent symbols for frequency-hopping multiple access," *IEEE Trans. Commun.* **45**(4), 408–410 (1997).
11. A. A. Shaar and P. A. Davies, "A survey of one-coincidence sequences for frequency-hopped spread spectrum systems," *IEE Proc. F, Commun. Radar Signal Process.* **131**(7), 719–724 (1984).
12. M. Azizoglu, J. A. Salehi, and Y. Li, "Optical CDMA via temporal codes," *IEEE Trans. Commun.* **40**(7), 1162–1170 (2002).

Elie Inaty received BS and MS degrees in electrical engineering from the University of Balamand, Lebanon, in 1996 and 1998, respectively. He received his PhD degree from Université Laval, Canada, in 2001. He is now an assistant professor at the University of Balamand and adjunct professor at Université Laval. His research interests include CDMA and WDM fiber optic communications, network control and resource management issues in optical communication networks, and radio multiple-access techniques.

Robert Raad received BS and MS degrees in computer engineering from the University of Balamand, El-Koura, North Lebanon. He received an award from the professors of the faculty of engineering at the University of Balamand in 2003. Currently, he is working toward his PhD at Laval University. His research interests include optical CDMA, network-control, and resource management issues in optical communications networks.

Paul Fortier received his BSc and MSc degrees in electrical engineering from Laval University, Québec, Canada, in 1982 and 1984, respectively, his MS degree in statistics, and his PhD degree in electrical engineering from Stanford University in 1987 and 1989, respectively. Since 1989, he has been with the Department of Electrical and Computer Engineering at Laval University, where he is currently a full professor. Since 2003, he has been the associate dean for development and research at the Faculty of Science and Engineering. His research interests include digital signal processing for communications and the study of complexity and performance tradeoffs in hardware implementations, with applications in wireless and optical communications. He has been involved in the organization of national and international conferences and workshops in these fields. He is a fellow of the Engineering Institute of Canada and a senior member of IEEE.

Hossam M. H. Shalaby received BS and MS degrees from the University of Alexandria, Egypt, in 1983 and 1986, respectively, and the PhD degree from the University of Maryland, College Park, in 1991, all in electrical engineering. In 1991 he joined the Department of Electrical Engineering, University of Alexandria, Egypt, as an assistant professor. He was promoted to associate professor in 1996 and to a professor in 2001 (current position). Since December 2000, he has been an adjunct professor with Department of Electrical and Information Engineering, Faculty of Sciences and Engineering, Laval University, Quebec, Canada. From September 1996 to January 1998, he was an associate professor with the electrical and computer engineering department at International Islamic University Malaysia, and from February 1998 to December 1998, he was with the School of Electrical and Electronic Engineering, Nanyang Technological University, Singapore, where he was a senior lecturer and from January 1999 to February 2001 as an associate professor. His research interests include optical communications, optical CDMA, spread-spectrum communications, and information theory.